Parametric Study of Low Frequency Broadband Rectilinear-to-Rotary Vibrational Energy Harvesting

Chen Jingfan[1], *Deng Wei*[2], *Wang Ya*[1*], *Inman Dan*[3]

1. Department of Mechanical Engineering, Stony Brook University, New York 11794, USA;
2. Department of Mechanical Engineering, Texas A&M University, Texas 77843, USA;
3. Department of Aerospace Engineering, University of Michigan, MI 48109, USA

(Received 6 December 2017; revised 18 January 2018; accepted 20 January 2018)

Abstract: A parametric study of a high-power-density dual resonator for achieving low frequency broadband electromagnetic energy harvesting is reported. The dual resonator consists of a rectilinear oscillator ($R_L O$) performing magnetic levitation and a rotary oscillator ($R_T O$) performing electromagnetic coupling through a stator and a rotor. Both oscillators, coupled by magnetic forces generated by a set of arc permanent magnets, radially magnetized and centro-symmetrically fixed onto the $R_L O$ and the rotor of the $R_T O$ achieve the reciprocating-to-rotary motion conversion and frequency up-conversion. Specifically, the dual resonator is able to convert stochastic reciprocating motion into controllable rotation, provide intrinsic frequency up-conversion, use non-contact magnetic coupling to provide near loss-free energy transfer and be configured into specific applications to obtain and maintain high-energy orbits of multi-stable energy harvesting. While solely focusing on developing a dual resonator provides substantial benefits, its dynamic behavior is unclear, thus electromagnetic-dynamic governing equations are derived, and a curve fitting model of restoring torque of $R_T O$ under different repulsive magnets configurations are developed to predict key characteristics and to improve performance of the electromechanical system. Power analysis is carried out for providing a quantitative guidance of customizing the harvester to achieve an optimal power density.

Key words: curve fitting model; non-contact rectilinear-to-rotary motion transformation; frequency up-conversion; systematic modeling; parametric study

CLC number: TM619; TN929 **Document code**: A **Article ID**: 1005-1120(2018)01-0001-09

0 Introduction

Despite the abundance of ambient vibrations, conventional linear rectilinear energy harvesters have notoriously limited efficiency[1], as they typically only work efficiently in a narrow band of frequencies centered around their own natural frequency, which reduces their power density. To widen the output bandwidth, active tuning mechanisms have been developed that adjust the natural frequency of the harvesters in response to the excitation frequency[2,3]. Study on circuit design for energy harvesters using switching techniques to increase harvesting efficiency have also been done[4,5]. For instance, the self-powered synchronized switching interface can extend the effective bandwidth by four times.

Another popular approach is to enable nonlinearity of the energy harvesters to obtain high-energy orbits by introducing external magnetic forces. The so-called nonlinear energy harvesters (NEHs), could be designed as softening or hardening configurations to widen output bandwidth under excitations with slowly varying frequencies[6]. Multiple cantilever beams with different but close natural frequencies have been also integrated to achieve broad bandwidth[7-9] but there is no interaction between these cantilever beams. To explore the interaction effect on the broadband output, two degree-of-freedom (2DOF) harvest-

* Corresponding author, E-mail: ya. s. wang@stonybrook. edu.

How to cite this article: Chen Jingfan, Deng Wei, Wang Ya, et al. Parametric study of low frequency broadband rectilinear-to-rotary vibrational energy harvesting[J]. Trans. Nanjing Univ. Aero. Astro., 2018,35(1):1-9.
http://dx. doi. org/10. 16356/j. 1005-1120. 2018. 01. 1

ers have been constructed[10-13] to have double resonant peaks and increased frequency bandwidth.

These aforementioned approaches can also be combined, such as using magnetic forces to couple two cantilever beams, and to form a nonlinear 2DOF energy harvester[14,15]. Experimental investigation has shown a nearly 100% increase in the operating bandwidth and a 41% increase in the magnitude of the power output at an excitation level of 2 m/s^2[15]. Such nonlinear energy harvesters could make the resonant peaks commensurable with suitable parameters, which results in more resonant peaks and wider bandwidth. Experiments have demonstrated a 130% increase in the bandwidth in comparison to their linear counterparts at an excitation level of 2 m/s^2[16].

However, the efficiency of NEHs is still much lower than rotary generators[17]. Rotary generators, generally outperform rectilinear devices, owning to concentrated magnetic flux variation in the coil. While they are particularly well suited for low-frequency, large-amplitude oscillations, the application of rotary generators is restricted to purely rotational energy sources, e. g. , wind turbines and hydroelectric stations.

A rectilinear-to-rotary motion conversion mechanism can address these shortcomings from both the rectilinear and the rotary nonlinear energy harvesters, and thus to provide an efficient approach to harvest low-frequency rectilinear vibrations. However, rectilinear-to-rotary motion conversion is traditionally achieved by using a combination of mechanical transmission components, such as crank and connecting rod or eccentric and pitman arm[18,19]. Not withstanding their benefits, the complex mechanical transmission components required for coupling, and the introduced excessive volume, mass, wear, friction, and energy loss, present significant challenges to reliability and durability. In most of these aforementioned approaches, friction and inelastic deformation lead to significant energy loss.

This paper reports a contactless dual resonator for achieving high-power-density low frequency broadband energy harvesting, consisting of a rectilinear oscillator and a rotary oscillator coupled through magnetic forces. We derived the electromagnetic-dynamic governing equations of the nonlinear 2DOF system. The combination of restoring torques produced by the interaction of repulsive magnets and ferromagnetic screws with arc magnets can enable the dual resonances to be tuned for different vibration sources. Thus, a curve fitting model of the restoring torque under different configurations is developed for future simulation of the system. Furthermore, the experimental results for harvested power are presented to confirm the power harvesting capacity.

1 Structural Design

The dual resonator (Fig. 1) builds off our previous work[20], consisting of a rectilinear oscillator ($R_L O$) performing magnetic levitation and a rotary oscillator ($R_T O$) performing electromagnetic coupling through a stator and a rotor. Both oscillators, coupled by magnetic forces generated by a set of arc permanent magnets (N52, 15 mm o. r. × 5 mm i. r. × 10 mm, 90°), radially magnetized and centro-symmetrically fixed onto the $R_L O$ and the rotor of the $R_T O$ achieve the reciprocating-to-rotary motion conversion and frequency up-conversion. Without the repulsive magnets, the magnetic interaction between the eight ferromagnetic screws and the rotor generates eight angular equilibrium positions (0, $\pi/4$, $2\pi/4$, $3\pi/4$, π, $5\pi/4$, $6\pi/4$ and $7\pi/4$). Two repulsive rectangular magnets (8 mm × 8 mm × 8 mm) are attached in the stator in $R_T O$ (Fig. 1(a)) to reduce the number of equilibrium positions from eight to four, and to shallow the potential well. The stator also has six coils (2 000 turns, 50 Ω). For each coil, a ferromagnetic screw is inserted inside to increase the magnetic flux cross the coil and it generates magnetic interaction with the magnets on the rotor, which along with the two repulsive magnets creates the desired potential well distribution.

The equivalent mechanical model of the harvester is presented schematically in Fig. 1(b). The governing equations of the nonlinear 2DOF

system subjected to base excitation F_{exc} can be described by

$$\begin{cases} m\ddot{z} + c_1\dot{z} = F_{exc} + F(\theta, z) - F_f - mg \\ I\ddot{\theta} + \left(c_2 + \dfrac{k_u^2 \sin^2(4\theta)}{R_{int} + R_L}\right)\dot{\theta} = M_r(\theta) + \tau(\theta, z) \\ V_{out} = \dfrac{k_u R_L \sin(4\theta)\dot{\theta}}{R_{int} + R_L} \end{cases} \quad (1)$$

where z, m and c_1 are the displacement, mass and damping coefficient of the $R_L O$, respectively; F_{exc} the input excitation force; F_f the friction force on $R_L O$ from the steel shafts; θ, I and c_2 the angular displacement, angular mass and damping coefficient of the $R_T O$, respectively; k_u the constant coefficient about electromechanical coupling; R_L the load resistance; R_{int} the internal resistance of the harvester; V_{out} the output voltage caused by the varied electromagnetic field; $F(\theta, z)$ and $\tau(\theta, z)$ the magnetic force and torque between the $R_L O$ magnet and the rotor magnets, and M_r the restoring torque generated by repulsive magnets and ferromagnetic screws on $R_T O$.

Eq. (1) shows that the angular displacement and angular acceleration has significant effect on the output voltage. The functions of $F(\theta, z)$ and $\tau(\theta, z)$ have been developed in our previous work[21]. In order to predict the response of the system, it becomes necessary to figure out how the restoring torque M_r produced by the interaction of arc magnets with repulsive magnets and attractive ferromagnetic screws result in a change in the rotational motion. So, the following section will derive the analytical model of the restoring torque on $R_T O$.

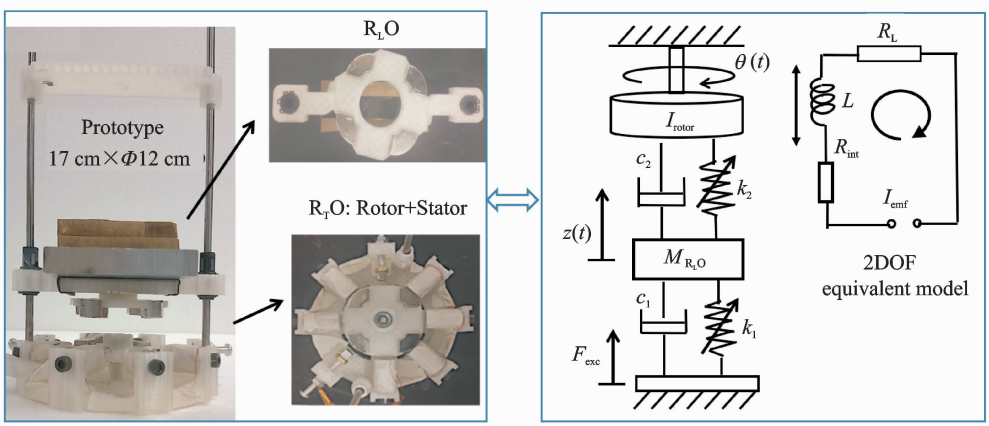

(a) Photographic representation of energy harvester

(b) Mechanical schematic of the proposed system and its equivalent circuit representation

Fig. 1 Structural design and mechanical schematic

2 Restoring Torque of $R_T O$: Parametric Study and Analysis

2.1 Experimental measurement

The restoring torque M_r was decided by the positions and quantities of repulsive magnets. To accurately describe the nonlinear characteristics of the energy harvester, the accurate nonlinear restoring torque M_r on rotor is needed. Since the size of arc magnets and repulsive magnets cannot be ignored compared with the distance between them, the Gilbert model[22] or the Ampère model[23] which assumes the permanent magnet as either a magnetic charge or magnetic dipole is not suitable for the system. Therefore, curve fitting method was used to derive the expression of M_r acted on the rotor from measurement data. As shown in Fig. 2, the stator of the rotary oscillator was fixed to a platform. By adjusting the side knob, the platform could rotate a certain angle. One end of a bar was fixed to the center of rotor, another end to the tip of the force sensor. The force corresponding to the angle can be read by the force sensor. By multiplying the force and the distance, the torque M_r could be calculated. d is the normal distances from the surface of repul-

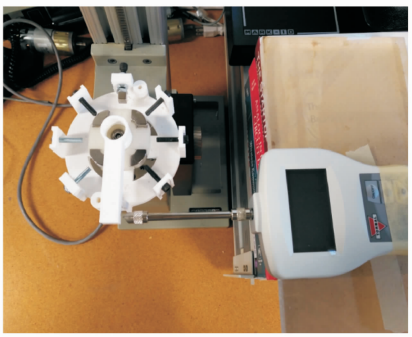

(a) Torque measurement setup

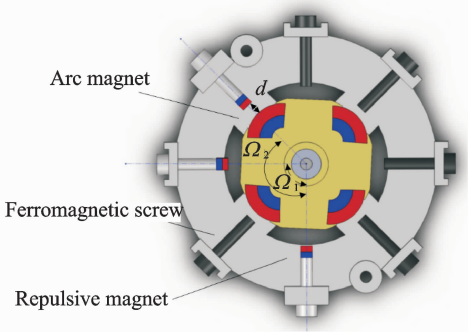

(b) Schematic of the arrangement of magnets

Fig. 2 Experimental setup of restoring torque measurement

sive magnets to the outer surface of the $R_T O$ magnets. Ω is the angle between two repulsive magnets.

2.2 Modeling and systematic analysis

The restoring torque M_r measured at any point on the $R_T O$ is a combination of torques generated by the interaction of repulsive magnets (T_{rep}) and arc magnets as well as attractive ferromagnetic screw (T_{scr}) and arc magnets. These torques are superimposed on each other. First, the repulsive torque function (T_{rep}) at different distance d when only one repulsive magnet was attached is needed to obtain. The torques at $d=$ 3.5, 3.9, 4.9, 5.3, 6.0 and 7.5 mm were measured and plotted in Fig. 3. Curve fitting was used to characterize the nonlinear restoring torque. The common function of the torque can be expressed as

$$T_{rep}(\theta)=A\sin(4\theta)+B\sin(8\theta) \tag{2}$$

with different coefficients A and B, which are dependent on the distance d.

By linear fitting A and B, as shown in Fig. 4, we have

$$\begin{cases} A(d)=15.04d-169.19 \\ B(d)=8.552\ 4d-82.74 \end{cases} \tag{3}$$

The same procedure was conducted to measure the torque produced by one attractive ferromagnetic screw, experimental result and curve fitted is shown in Fig. 5.

Thus, the equation of torque (T_{scr}) can be expressed as the following equations in one period ($\pi/2$)

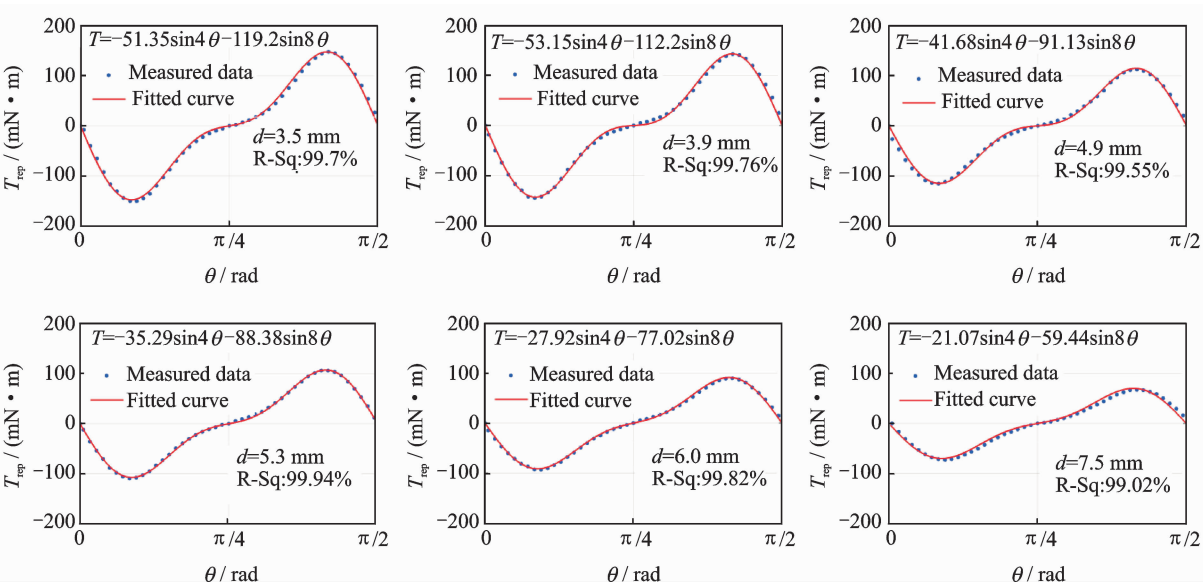

Fig. 3 Restoring torques when only one magnet was applied at different distances(T_{rep})

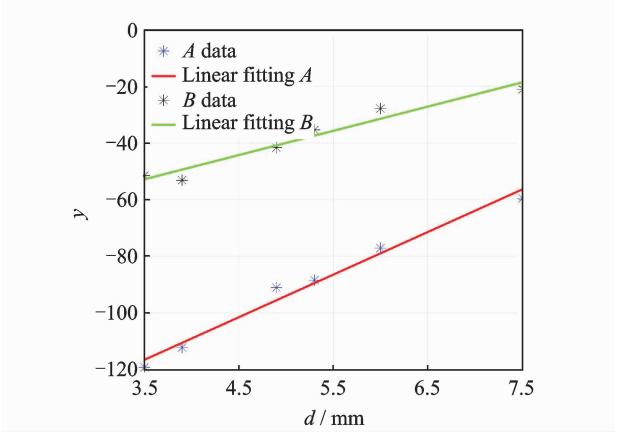

Fig. 4 Linear fitting of coefficients A and B

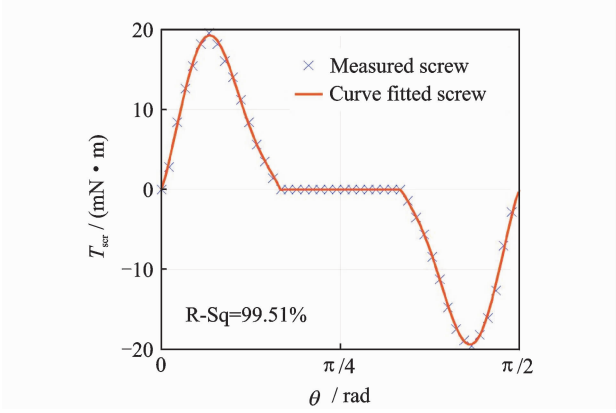

Fig. 5 Curve fitted of torque given by ferromagnetic screw (T_{scr})

$$\begin{cases} T_{scr}(\theta)=16.7\sin(5.875\theta+0.1572)+3.018\sin(15.665\theta-1.402) & \theta\in\left[0,\dfrac{\pi}{6}\right] \\ T_{scr}(\theta)=0 & \theta\in \text{Other values} \\ T_{scr}(\theta)=16.7\sin(5.875\theta+3.189)+3.018\sin(15.665\theta+2.056) & \theta\in k\left[\dfrac{\pi}{3},\dfrac{\pi}{2}\right] \end{cases} \quad (4)$$

The comprehensive restoring torque M_r is the combination of torques generated by repulsive magnets and ferromagnetic screws, which gives

$$M_r(\theta)=\sum T_{rep}(i)+T_{scr}(j) \quad i+j=8 \quad (5)$$

Simulated the torque for different configurations of repulsive magnets by using equation M_r, as shown in Fig. 6, the simulation results agree well with the experimental results no matter the number of repulsive magnets or varied distance d were applied demonstrating the validity of our fitted equations.

In this section, we created a systematic model

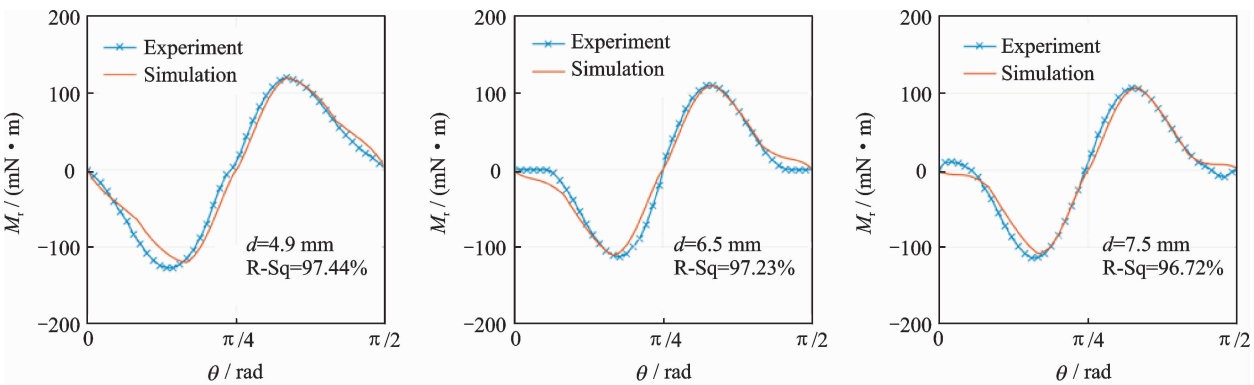

(a) One repulsive magnet and seven screws applied

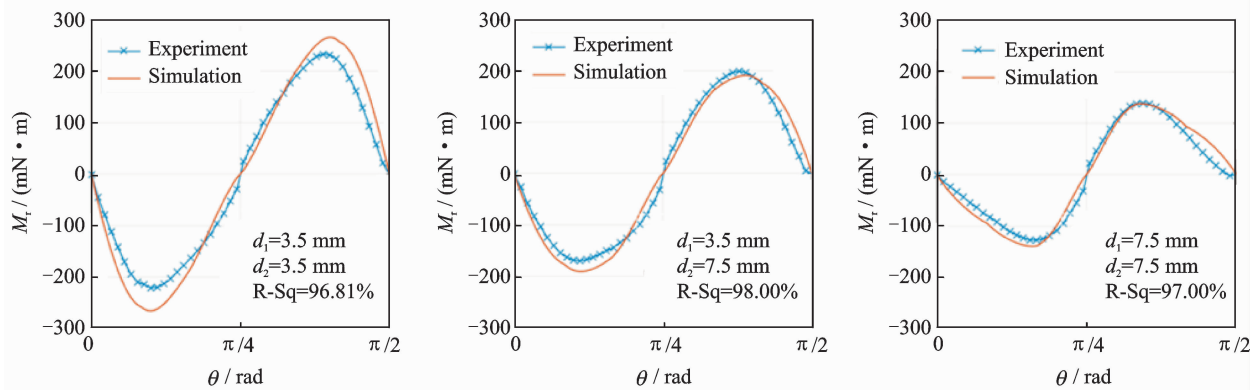

(b) Two repulsive magnets and six screws applied with $\Omega=90°$

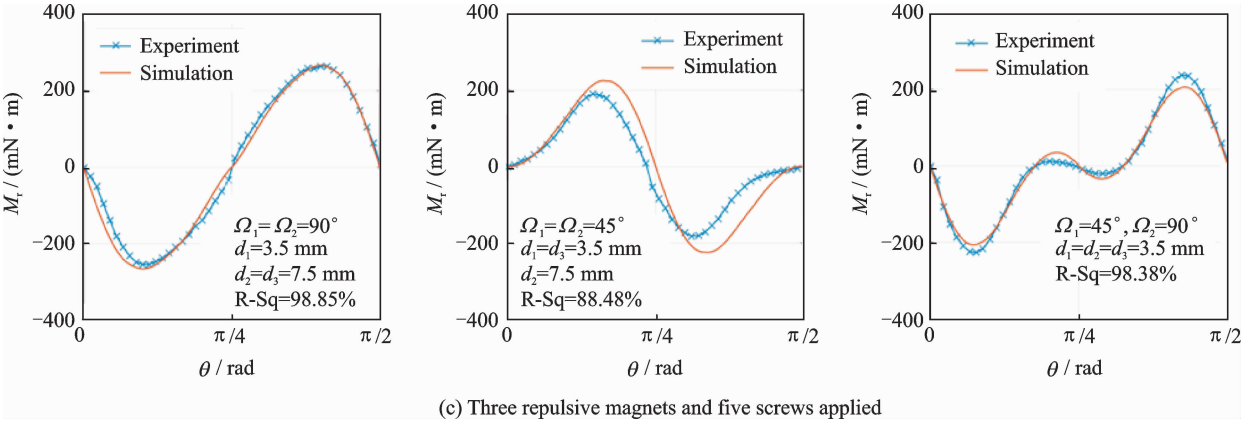

Fig. 6 Experimental and simulation results of the restoring torque (M_r)

of the restoring torque (M_r), whose waveform has approximated sinusoidal dependence on the rotor angular displacement. By adding the repulsive magnets, the number of equilibrium positions can be reduced from 8 to 4, that is, the period of restoring torque changes with the presence of repulsive magnet(s): $\pi/4$ without magnet and $\pi/2$ with magnet, respectively. Through experimental verification, the curve fitting model can accurately describe the restoring torque of $R_T O$ under different repulsive magnets configurations, which will benefit for predicting the response of the dual resonator system.

3 Power Output Analysis

To illustrate the behavior of the energy harvester, excite this system at different frequency to move the $R_L O$ upward or downward the $R_T O$, thereby producing a repulsive torque to push the rotor oscillate at a certain degree and then the rotor will swing back due to the potential energy well. As shown in Fig. 7, a long stroke electrodynamic shaker (APS dynamics Inc.) is controlled by a signal generator (KEYSIGHT 33500B) in conjunction with a power amplifier (APS 125) to provide a sine excitation with various frequencies acted on the prototype harvester. A piezo accelerometer (PCB333B32) measures the input excitation level and a laser sensor (optoNCDT1402, Micro-Epsilon Inc.) measures the rectilinear displacement of the $R_L O$.

Fig. 8 shows the time history plot of the

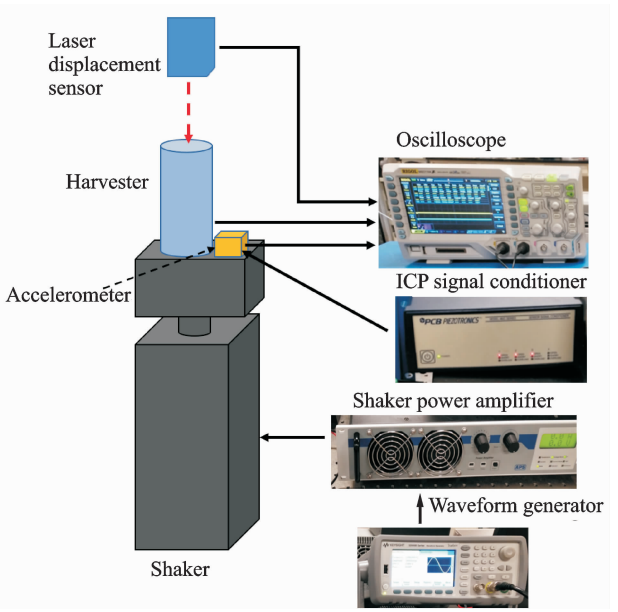

Fig. 7 Schematic diagram of the experimental setup

open-circuit voltage and corresponding $R_L O$ displacement at different with one repulsive magnets ($d=3.5$ mm), Fig. 8(a), and two repulsive magnets ($d_1=3.5$ vmm, $d_2=7.5$ mm, $\Omega=135°$), Fig. 8(b), attached. One magnet has a higher and denser voltage output than two magnets due to the larger restoring torque which result in a deeper potential energy well. However, the shallow potential energy well (two magnets) results in a wider bandwidth. For one magnet configuration, it was also found that with input excitations being at low frequencies, the driving magnet might get stuck and does not pluck the rotor effectively. With a higher input frequency (5—7 Hz), the $R_L O$ is able to drive the rotor to escape potential energy wells with a high angular velocity. The

rotor oscillates over equilibrium positions for several vibration cycles periodically and generates output voltage at larger amplitude. However, when the input frequency is larger than 7 Hz, due to the small amplitude rectilinear motion, the $R_L O$ does not have strong magnetic interaction with the rotor. Therefore, the output voltage is small. The frequency-up conversion is observed when the $R_L O$ drives the rotor to escape potential wells, and the subsequent driving torque starts to deflect the rotor before the resonant vibration induced by the previous torque had fully run down.

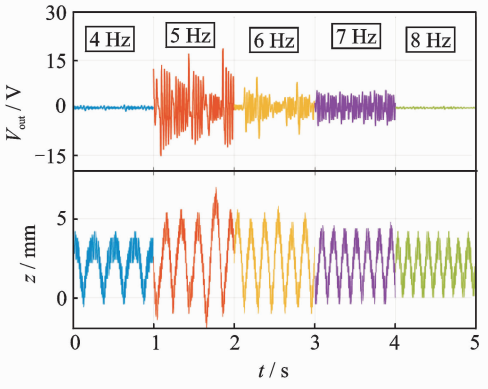

(a) One repulsive magnet with d=3.5 mm

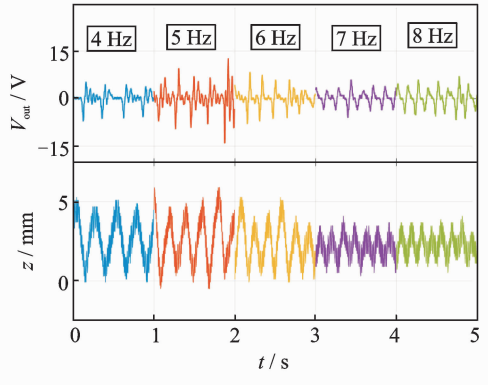

(b) Two repulsive magnets with d_1=3.5 mm, d_2=7.5 mm, Ω=135°

Fig. 8 Experimental output voltage and $R_L O$ displacement under different input frequencies and 0.5g acceleration

Fig. 9 shows the frequency responses of the open circuit voltage against excitation frequencies ranged from 2 Hz to 10 Hz under 0.5g base accelerations. One repulsive magnet configuration has a denser output voltage and most voltages are achieved at 4—7.5 Hz range. Two repulsive magnets configuration has a wider operation bandwidth from 4 Hz to 8 Hz.

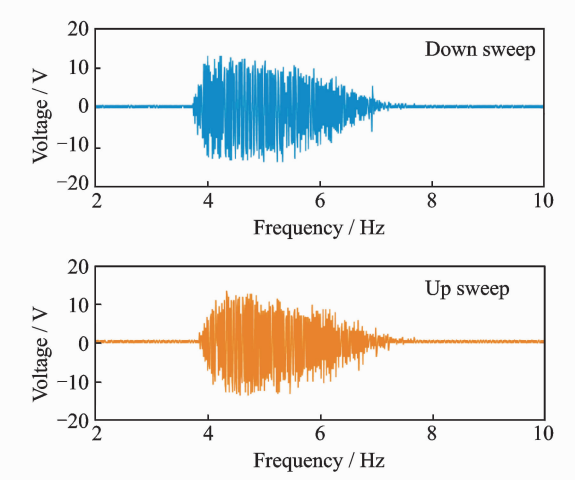

(a) One repulsive magnet with d=3.5 mm

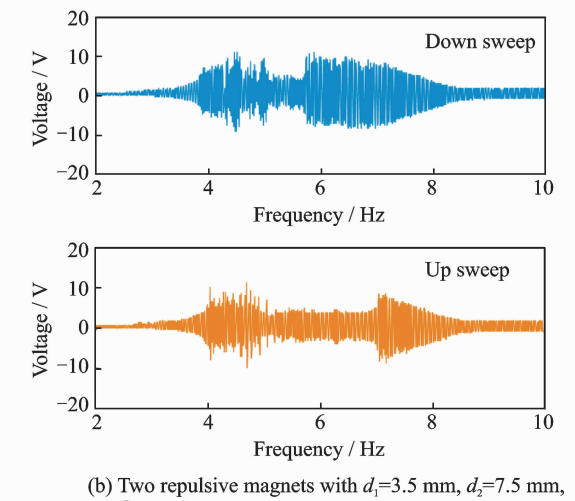

(b) Two repulsive magnets with d_1=3.5 mm, d_2=7.5 mm, Ω=135°

Fig. 9 Frequency sweep of output voltage at 0.5g acceleration

A tunable resistor was connected between the electrodes of the harvester to experimentally determine the optimal load-resistance for maximum power output when one repulsive magnets (d=3.5 mm) was attached. The value R_L of the resistor and voltage V_R across the load were measured. The instantaneous power delivered by the energy harvester can be obtained according to $P=V_R^2/R_L$. Fig. 10 shows the experimental results of output RMS power and RMS voltage, normalized by the base acceleration, versus load resistance. The maximum output RMS power is 183 m W/g^2 at the resistive load of 500 Ω, which is three times larger than our previous work.

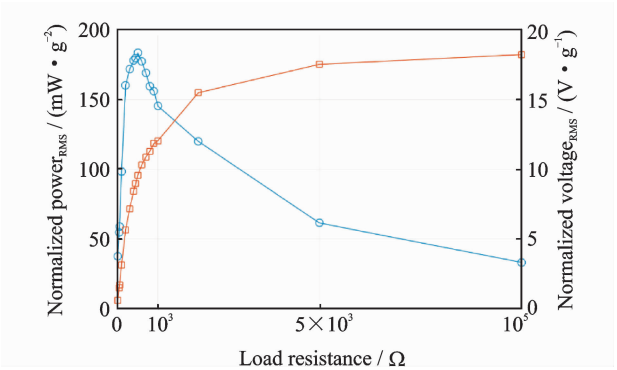

Fig. 10 Experimental measurement of RMS power output and RMS voltage output under harmonic excitation of 5 Hz at 0.5g

4 Conclusions

This paper reports a contactless high-power-density energy harvester energy was harvested using coils and magnets by converting stochastic reciprocating motion into controllable rotation, to provide intrinsic frequency up-conversion, and to be configured into specific applications to obtain and maintain high-energy obits of multi-stable energy harvesting with near-unity energy conversion efficiency and bandwidth widening. A parametric study is also presented to underlie the dynamic mechanisms of the prototype, a curve fitting model of restoring torque was developed, and a reliable approach is proposed to estimate the magnetic interaction for given configurations, which can be used for predicting response of the electromechanical system. The experiment power analysis demonstrated the up-conversion of a 5 Hz input excitation into an output voltage with a frequency of about 30 Hz, which is six times the input frequency. The maximum output RMS power is 183 mW/g^2 at the resistive load of 500 Ω, which is three times larger than our previous work.

Acknowledgements

This work was partially supported by the U. S. Office of Navy Research (No. N000141410230), and partially supported by the Department of Energy ARPA-E (No. DOE-AR0000531).

References:

[1] WDENG, WANG Y. Input-dependent performance study of a nonlinear piezoelectric energy harvester [J]. Journal of Intelligent Material Systems and Structures, 2016. doi: 10.1177/0123456789123456.

[2] LELAND E S, WRIGHT P K. Resonance tuning of piezoelectric vibration energy scavenging generators using compressive axial preload[J]. Smart Materials and Structures, 2006. 15(5):1413.

[3] CHALLA V R, PRASAD M, SHI Y, et al. A vibration energy harvesting device with bidirectional resonance frequency tunability[J]. Smart Materials and Structures, 2008, 17(1):015035.

[4] SHIH Y S, VASIC D, WU W J. A non-contact mechanical solution for implementing synchronized switching techniques for energy harvesting using reed switches[J]. Smart Materials and Structures, 2016, 25(12):125013.

[5] LALLART M. Nonlinear technique and self-powered circuit for efficient piezoelectric energy harvesting under unloaded cases[J]. Energy Conversion and Management, 2017, 133:444.

[6] STANTON S C, MCGEHEE C C, MANN B P. Reversible hysteresis for broadband magnetopiezoelastic energy harvesting [J]. Applied Physics, 2009, 95 (17):174103.

[7] SHAHRUZ S. Design of mechanical band-pass filters for energy scavenging[J]. Journal of Sound and Vibration, 2006, 292(3):987.

[8] FERRARI M, FERRARI V, GUIZZETTI M, et al. Piezoelectric multifrequency energy converter for power harvesting in autonomous microsystems[J]. Sensors and Actuators A: Physical, 2008, 142(1): 329.

[9] XUE H, HU Y, WANG Q M. Broadband piezoelectric energy harvesting devices using multiple bimorphs with different operating frequencies[J]. Ultrasonics, Ferroelectrics, and Frequency Control, IEEE Transactions on, 2008, 55(9): 2104.

[10] ZHOU W, PENAMALLI G R, ZUO L. An efficient vibration energy harvester with a multi-mode dynamic magnifier [J]. Smart Materials and Structures, 2011, 21(1):015014.

[11] ALADWANI A, ARAFA M, ALDRAIHEM O, et al. Cantilevered piezoelectric energy harvester with a dynamic magnifier[J]. Journal of Vibration and Acoustics, 2011, 134(3):031004.

[12] KIM I, JUNG H, LEE B M S. Broadband energy-harvesting using a two degree-of-freedom vibrating

body[J]. Applied Physics Letters, 2011, 98(21): 214102.

[13] CHEN S J, WU J Y. Fabrication of a 2-DoF electromagnetic energy harvester with in-phase vibrational bandwidth broadening [J]. Smart Materials and Structures, 2016, 25(9): 095047.

[14] ZHOU S, CAO J, WANG W, et al. Modeling and experimental verification of doubly nonlinear magnet-coupled piezoelectric energy harvesting from ambient vibration[J]. Smart Materials and Structures, 2015, 24(5): 055008.

[15] TANG L, YANG Y. A nonlinear piezoelectric energy harvester with magnetic oscillator[J]. Applied Physics Letters, 2012, 101(9): 094102.

[16] XIONG L, TANG L, MACE B R. Internal resonance with commensurability induced by an auxiliary oscillator for broadband energy harvesting[J]. Applied Physics Letters, 2016, 108(20): 203901.

[17] DENG W, WANG Y. Low frequency energy harvesting with contactless-coupled rectilinear-rotary oscillations mediated by magnetic interaction towards frequency up-conversion and wider bandwidth[J]. Applied Physics Letters, 2012(101): 094102.

[18] DENG W, WANG Y. Apparatus and method for harvesting electromagnetic energy from low frequency vibration using rectilinear oscillator coupled to rotary counterpart: US62376169[P]. 2016.

[19] DENIJS J F, Lindner M. Transmission for converting rotary motion into linear motion: US5690567 A [P]. 1997.

[20] BAUER F. Device for converting rectilinear motion into rotary motion: US3279269 A[P]. 1966.

[21] DENG W, WANG Y. Non-contact magnetically coupled rectilinear-rotary oscillations to exploit low frequency broadband energy harvesting with frequency up-conversion[J]. Applied Physics Letters, 2016, 109(14): 133903. 10. 1063/1. 4963786.

[22] DENG W, WANG Y. A dual resonant rectilinear-to-rotary oscillation converter for low frequency broadband electromagnetic energy harvesting[J]. Smart Materials and Structures, 2017, 26(9): 095059.

[23] AKOUN G, YONNET J P. 3D analytical calculation of the forces exerted between two cuboidal magnets [J]. IEEE Transactions on Magnetics, 1984. 20(5): 1962-1964.

[24] YUNG K W, LANDECKER P B, VILLANI D D. An analytic solution for the force between two magnetic dipoles[J]. Magnetic and Electrical Separation, 1998, 9(1): 39-52.

Ms. **Chen Jingfan** received the B. S. degree in materials forming and control Engineering from Harbin Institute of Technology at Weihai in 2014 and the M. S. degrees in industrial engineering from Texas A&M University-Kingsville in 2016. She is currently pursuing the Ph. D. degree in mechanical engineering at Stony Brook University. Her research work is focusing on vibrational energy harvesting.

Mr. **Deng Wei** received the B. S. and the M. S degrees in mechanical engineering from University of Science and Technology of China in 2014 and Stony Brook University in 2016, respectively. Now he is pursuing the Ph. D. degree in mechanical engineering at Texas A&M University.

Prof. **Wang Ya** is currently an assistant professor in mechanical engineering at Stony Brook University. She received the B. S. degree mechatronics from Shandong University in 2004, the M. S. degree in mechanical engineering, University of Puerto Rico in 2007, and the Ph. D. degree in mechanical engineering from Virginia Polytechnic Institute and State University in 2012. Her research interests include smart materials and structures applied to sensing, energy harvesting, and vibration control. She is a member of ASME, IEEE, AIAA and SPIE, and serves as an elected member of technical committees of ASME Aerospace Division, Adaptive Structures and Material Systems Branch.

Prof. **Inman Dan** is the Clarence "Kelly" Johnson Collegiate Professor and Department Chair of Aerospace Engineering at the University of Michigan. He received his Ph. D. degree from Michigan State University in Mechanical Engineering in 1980. He works in the area of applying smart structures to solve aerospace engineering problems including energy harvesting, structural health monitoring, vibration suppression and morphing aircraft. He is a Fellow of AIAA, ASME, IIAV, SEM and AAM.

(Production Editor: Zhang Tong)